Fractals, Vol. 14, No. 3 (2006) 231–243

World Scientific
www.worldscientific.com

SCALING PROPERTIES OF THE SPREAD HARMONIC MEASURES

DENIS S. GREBENKOV
Laboratoire de Physique de la Matière Condensée
UMR 7643, C.N.R.S.–Ecole Polytechnique
Route de Saclay, 91128 Palaiseau Cedex, France
denis.grebenkov@polytechnique.edu

Received December 19, 2004
Accepted December 14, 2005

Abstract

A family of the spread harmonic measures is naturally generated by partially reflected Brownian motion. Their relation to the mixed boundary value problem makes them important to characterize the transfer capacity of irregular interfaces in Laplacian transport processes. This family presents a continuous transition between the harmonic measure (Dirichlet condition) and the Hausdorff measure (Neumann condition). It is found that the scaling properties of the spread harmonic measures on prefractal boundaries are characterized by a set of multifractal exponent functions depending on the only scaling parameter. A conjectural extension of the spread harmonic measures to fractal boundaries is proposed. The developed concepts are applied to give a new explanation of the anomalous constant phase angle frequency behavior in electrochemistry.

Keywords: Spread Harmonic Measure; Fractals; Scaling; (Partially) Reflected Brownian Motion; Mixed Boundary Condition.

1. INTRODUCTION

Scaling properties of various measures on fractal sets have fascinated both physicists and mathematicians for a long time.[1–4] The harmonic measure is probably the most known example in physics. Providing a powerful mathematical tool to characterize the accessibility of an irregular interface by Brownian motion, it is involved in growth processes (like diffusion limited aggregation or dendric growth[5,6]), in electrostatic problems (charge

distribution on a metallic surface[7]), or in diffusional transport (primary flux or current distribution[8–10]). For a given domain Ω with boundary $\partial\Omega$, the harmonic measure $\omega_x\{A\}$ of a subset $A \subset \partial\Omega$ is defined as the probability that the Brownian motion started from a fixed interior point $x \in \Omega$ hits the boundary $\partial\Omega$ on the subset A for the first time. Being defined on a fractal set, the harmonic measure exhibits non-trivial scaling properties, so-called *multifractal behavior*, that have been studied thoroughly (see Meakin[3] and references therein). The other well-known example is the Hausdorff measure extending the notion of volume to fractal sets.

The particular interest to the harmonic and Hausdorff measures is based on their direct relation to the Dirichlet and Neumann boundary conditions. According to the Kakutani theorem,[11] the harmonic measure $\omega_x\{A\}$, considered as a function of x, solves the following Dirichlet-Laplace problem:

$$\begin{aligned} \Delta\omega_x\{A\} &= 0 \qquad (x \in \Omega), \\ \omega_x\{A\} &= \mathbb{I}_A(x) \quad (x \in \partial\Omega) \end{aligned} \tag{1}$$

where Δ is the Laplace operator, and $\mathbb{I}_A(x)$ stands for the indicator function of subset A (i.e. $\mathbb{I}_A(x) = 1$ for $x \in A$ and $\mathbb{I}_A(x) = 0$ otherwise). In a physical point of view, the harmonic measure is related to a *purely absorbing* boundary (Dirichlet condition): when a diffusing particle hits the boundary, it is immediately absorbed (or transferred through the boundary). If now one considers a *purely reflecting* boundary (Neumann condition), the diffusing particle will never leave the domain. After a number of reflections from the surface, the particle "forgets" its anterior trajectory and can be found in a vicinity of any boundary point, whatever its initial starting position. Such a uniform probability distribution corresponds to the Lebesgue measure on a smooth boundary or to the Hausdorff measure on a fractal set.

When one deals with a real physical or chemical transport process, the reflecting and absorbing interfacial effects are present simultaneously and can be mathematically described via the *mixed boundary condition*. In order to characterize the spatial distribution of absorptions on such *semi-permeable* interface, one can introduce a family of the *spread harmonic measures* parametrized by a positive parameter Λ homogeneous to the length.[12] For a given subset A of a smooth boundary $\partial\Omega$, these measures can be formally constructed as the solutions of the mixed boundary value problem:

$$\begin{aligned} \Delta\omega_{x,\Lambda}\{A\} &= 0 \qquad (x \in \Omega), \\ \left[I - \Lambda\frac{\partial}{\partial n}\right]\omega_{x,\Lambda}\{A\} &= \mathbb{I}_A(x) \quad (x \in \partial\Omega) \end{aligned} \tag{2}$$

where I stands for the identity operator, and $\partial/\partial n$ is the normal derivative directed towards the interior of the domain. The operator in square brackets at the second relation in (2) presents a linear combination of the Dirichlet and Neumann boundary conditions. The positive parameter Λ controls the "ratio" between reflections and absorptions on the boundary: $\Lambda = 0$ corresponds to a perfectly absorbing boundary (Dirichlet condition), while $\Lambda = \infty$ represents a perfectly reflecting boundary (Neumann condition). This parameter is usually related to the physical or chemical properties of the bulk and the interface that provides a way to apply the present harmonic analysis in different fields. Examples of the transport phenomena where partial absorptions and reflections are involved can be found in physiology (oxygen diffusion towards and across alveolar membranes in the pulmonary acinus[13,14]), in electrochemistry (electric transport through metallic electrodes placed into electrolyte[8,9,15]), or in petrochemistry (diffusion of reactive molecules towards catalytic surface[16,17]). In all these cases, the geometrical irregularity of the interface is omnipresent and known to be crucial. Consequently, the scaling behavior of the spread harmonic measures on such irregular boundaries turns out to be the key point in understanding these phenomena.

The paper is organized as follows. First, we recall basic definitions related to the spread harmonic measures. We then discuss the spreading effect of partial reflections and the role of the parameter Λ. The scaling properties of the spread harmonic measures will be obtained by means of qualitative arguments and then justified by numerical simulations. As a physical application of these results, a new explanation of the anomalous constant phase angle (CPA) frequency behavior of the spectroscopic impedance is proposed. The paper will be closed by a conjectural extension of the spread harmonic measures to the case of really fractal boundaries.

2. DEFINITION AND BASIC PROPERTIES

In this section, we briefly recall the definition and basic properties of the spread harmonic measures.[12]

In order to clarify the underlying concepts, we begin with an intuitive construction inspired by partially reflected random walks.[10] A more formal and rigorous definition will then be given.

2.1. Intuitive Construction

For a given domain $\Omega \subset \mathbb{R}^d$ with a smooth boundary $\partial\Omega$, let us consider the stochastic process which can be called *Brownian motion reflected with jump*. The (ordinary) Brownian motion starts from a fixed interior point $x \in \Omega$. When it hits the boundary $\partial\Omega$ at some point s, two complementary events may happen:

- with a given sticking probability σ, the motion is terminated (absorbed) on the boundary $\partial\Omega$;
- or, with probability $(1-\sigma)$, it is reflected by a jump to the neighboring point $s + an(s)$, belonging to the domain Ω, where $n(s)$ is the inward unit normal to the boundary at point s, and a is a small positive parameter. From this point, the Brownian motion is being continued until the next hit to the boundary, and so on.

The distribution of the first hitting point s is given by the harmonic measure density $\omega_x(s)$. If the process is reflected after the first hit, it is continued from the interior point $s+an(s)$. Applying again the harmonic measure density, $\omega_{s+an(s)}(s')$, one determines the distribution of the second hitting point s', and so on. Since the Brownian motions before and after each reflection are independent by construction, the probability distribution of the last hitting point, where this stochastic process is finally absorbed, can be written as:

$$\begin{aligned}\omega^{(a)}_{x,\sigma}(s) = \sigma\omega_x(s) &+ \sigma(1-\sigma)\int_{\partial\Omega} ds_1 \\ &\times \omega_x(s_1)\ \omega_{s_1+an(s_1)}(s) \\ &+ \sigma(1-\sigma)^2 \int_{\partial\Omega}\int_{\partial\Omega} ds_1 ds_2 \\ &\times \omega_x(s_1)\ \omega_{s_1+an(s_1)}(s_2) \\ &\times \omega_{s_2+an(s_2)}(s) + \cdots .\end{aligned}$$

In this infinite sum, kth term represents the contribution of trajectories with $(k-1)$ reflections (see Refs. 12 and 18 for details).

For the above definition, it was important to have a strictly positive jump distance a. If one took $a = 0$, the Brownian motion could not leave the vicinity of the first hitting point, and all further reflections would happen at this point. As a consequence, one would simply obtain the harmonic measure density, whatever strictly positive value of the probability σ: $\omega^{(a=0)}_{x,\sigma}(s) \equiv \omega_x(s)$. A non-trivial result can be found only in the double limit when both the jump distance a and the sticking probability σ vanish simultaneously. The mixed boundary condition leads to the following relation:[10,19]

$$\sigma = (1 + \Lambda/a)^{-1} \approx a/\Lambda. \tag{3}$$

When the jump distance decreases, the Brownian motion after each reflection explores smaller and smaller regions of the boundary. Apparently, this effect is compensated by an increase of the average number of reflections. This qualitative reasoning allows to think that densities $\omega^{(a)}_{x,\sigma}(s)$ converge to a non-trivial *spread harmonic measure density* $\omega_{x,\Lambda}(s)$ in the double limit when both a and σ go to 0, being related by (3).

2.2. Rigorous Definition

A rigorous definition of the spread harmonic measures was proposed in Grebenkov.[12] For a bounded domain $\Omega \subset \mathbb{R}^d$ with twice continuously differentiable boundary $\partial\Omega$, one can define two stochastic processes: the reflected Brownian motion $\hat{W}_t$ (started from a given point $x \in \Omega$) and the local time $\mathcal{L}_t$ on the boundary.[20,21] For a given positive parameter Λ, one introduces the stopping time $\mathbb{T}^x_\Lambda$ when the local time process $\mathcal{L}_t$ exceeds an exponentially distributed random variable χ (independent of $\hat{W}_t$ and $\mathcal{L}_t$):

$$\begin{aligned}\mathbb{T}^x_\Lambda &= \inf\{t > 0 : \mathcal{L}_t \geq \chi\} \\ &\text{where } \mathbb{P}\{\chi > \lambda\} = \exp[-\lambda/\Lambda].\end{aligned} \tag{4}$$

The stochastic process $\hat{W}_t$ conditioned to stop at random moment $t = \mathbb{T}^x_\Lambda$ is then called *partially reflected Brownian motion* (PRBM).

For a Borel subset $A \subset \partial\Omega$, one defines its spread harmonic measure $\omega_{x,\Lambda}\{A\}$ as the probability that the PRBM is stopped on A:

$$\omega_{x,\Lambda}\{A\} = \mathbb{P}\{\hat{W}_{\mathbb{T}^x_\Lambda} \in A\}.$$

One can show that the measure $\omega_{x,\Lambda}\{A\}$, considered as a function of x, solves the mixed boundary value problem (2) for a given parameter Λ. Since the boundary $\partial\Omega$ was assumed to be smooth, the spread harmonic measure density $\omega_{x,\Lambda}(s)$ is also well defined. It has been outlined in Grebenkov[12] that $\omega_{x,\Lambda}(s)$ turns out to be the limit of a sequence

of the absorption probability densities $\omega_{x,\Lambda}^{(a)}(s)$ as a goes to 0. In other words, the PRBM can be intuitively thought as a limit of the previously constructed Brownian motion reflected with jump when the jump distance a vanishes.

When $\Lambda = 0$, the random variable χ is equal to 0 with probability 1, i.e. the stopping time $\mathbb{T}_{\Lambda=0}^{x}$ describes the random moment when the local time $\mathcal{L}_t$ first exceeds 0. This is precisely the moment of the first hitting of the boundary. Consequently, one retrieves the definition of the (ordinary) harmonic measure for $\Lambda = 0$. For the opposite case of $\Lambda = \infty$, the probability for the random variable χ to have any finite value is formally equal to 0, and the reflected Brownian motion is never stopped. In this limit, the probability to find the reflected Brownian motion on subset A converges to its surface area divided by the surface area of the whole boundary. As a result, the family of the spread harmonic measures, parametrized by the positive parameter Λ, presents a continuous transition between the harmonic measure at $\Lambda = 0$ and the normalized Lebesgue measure at $\Lambda = \infty$. The last one will correspond to the Hausdorff measure for fractal sets.

3. SCALING PROPERTIES

In this section, we focus the attention on the scaling properties of the spread harmonic measures on finite generations of a deterministic self-similar fractal of Hausdorff dimension D_0 embedded in the two-dimensional plane $\mathbb{R}^2$. Such generations are typically composed of a finite number of smooth parts (e.g. linear segments). Although these prefractal curves are not differentiable at "connection" points between smooth parts, one can still proceed the construction of the Brownian motion reflected with jump since the probability to hit these particular points is equal to 0. As a generic boundary, one may think about a finite generation of the quadratic Koch curve constructed through an iterative procedure (Fig. 1).

The harmonic and Hausdorff measures exhibit their scaling properties even for *finite* generations of a fractal boundary. One can thus expect a similar behavior for the spread harmonic measures defined on a prefractal boundary of sufficiently high generation order. A non-trivial result that we are going to establish now is that the scaling behavior of the spread harmonic measures can be properly characterized by a set of the "multifractal exponent functions." Depending on the only scaling parameter, these functions turn out to be *intrinsic* characteristics of the spread harmonic measures on a given type of geometry, and thus they allow to proceed a *quantitative* multifractal analysis for different generation orders, length scales and values of the parameter Λ.

3.1. Spreading Effect

Partial reflections on the boundary lead to so-called *spreading effect*.[10] Arriving onto the boundary, the diffusing particle is not absorbed immediately, but it has to explore a certain interfacial region around the first hitting point due to multiple reflections from the surface. It yields *widening* or *spreading* of the harmonic measure controlled by the length Λ: larger values of Λ correspond to more spread harmonic measures, and vice versa. Indeed, as a parameter of the exponential law (4), the length Λ determines the "lifetime" of the partially reflected Brownian motion and, consequently, the average size of the interfacial region of the boundary which is explored between the first hit and the final absorption.

For a given domain Ω, let us introduce a *characteristic absorption region* (CAR) as a part of the boundary "around" the first hitting point such that its spread harmonic measure is equal to 1/2. For the two-dimensional case considered here, the boundary is an ordinary curve and the CAR is a curvilinear interval A centered at the first hitting point. For a given length Λ, its curvilinear perimeter L_{abs} is determined by the condition $\omega_{x,\Lambda}\{A\} = 1/2$. For

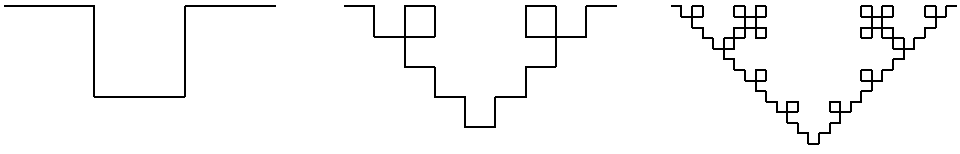

Fig. 1 Three generations of the quadratic Koch curve: at each iteration, one replaces all linear segments by the first generation (generator).

a flat boundary (linear segment or straight line), this perimeter has been calculated analytically by Grebenkov *et al.*[19] $L_{abs} \approx 1.246\ \Lambda$. This result provides a geometrical meaning of the parameter Λ as an estimate for the perimeter of the CAR. For an irregular boundary, L_{abs} depends on the first hitting point s. In the case of Koch type boundaries, it has been shown numerically by Grebenkov *et al.*[19] that this perimeter, averaged over all hitting points on the CAR, is still close to Λ (under condition that Λ is much less than the total perimeter L_{tot} of the boundary). More generally, we say that the boundary is *locally accessible* if, for a wide range of Λ, the averaged perimeter L_{abs} of the characteristic absorption region scales as Λ. In other words, the local accessibility condition means that the partially reflected Brownian motion started in a vicinity of a boundary point can reach any boundary point within a curvilinear distance Λ, with a relatively high probability. Figuratively speaking, there are no "hidden" boundary points which are difficult to access. The condition $\Lambda \ll L_{tot}$ is necessary since, whatever the boundary, the averaged perimeter L_{abs} does not exceed the total perimeter L_{tot}, while the parameter Λ can be freely increased up to infinity. Without pretence to a rigorous definition, the above qualitative notion of the local accessibility will be sufficient for the purposes of this paper.

A straight line and finite generations of the quadratic Koch curve are examples of locally accessible boundaries. It is also not difficult to construct an example when the local accessibility condition is not satisfied. Indeed, one can consider boundaries with "fjords" or deep pores characterized by very narrow entrances. Since the accessibility of the boundary points inside the "fjords" is very low, they can be thought as almost disconnected from the main "bay." If L_{fjord} denotes the total perimeter of such a "fjord," the averaged perimeter of the CAR inside the "fjord" will be of order of L_{fjord} (for $\Lambda \gg L_{fjord}$), while the averaged perimeter of the CAR in the main "bay" is still close to Λ. It allows to construct a geometry with any given ratio between the averaged perimeter L_{abs} of the characteristic absorption region and the parameter Λ.

Being naturally defined with the help of the spread harmonic measure, the notion of locally accessible boundary seems to be more general. In particular, similar concepts have been employed by Sapoval to develop the Land Surveyor Approximation (LSA) for transport phenomena.[8] Within this approach, the total flux across a *partially* absorbing boundary (mixed boundary condition) is approximated by the total flux across the new *perfectly* absorbing boundary (Dirichlet condition) obtained by coarse-graining with length Λ (see Fig. 2). In the light of the present work, the coarse-grain procedure corresponds to the replacement of the characteristic absorption regions (of the perimeter L_{abs} close to Λ) by perfectly absorbing linear chords (segments). Being reformulated in this way, the LSA found its mathematical justification. In particular, this approximation has to be valid for any locally accessible boundary, in agreement with numerical results by Filoche and Sapoval.[22]

Throughout this paper, the boundaries are assumed to be locally accessible, so that the averaged perimeter L_{abs} of the characteristic absorption region scales as Λ. Since we are going to study the *scaling* properties of the spread harmonic measures, a subtle difference between L_{abs} and Λ can be neglected. In what follows, L_{abs} and Λ will be identified.

3.2. Multifractal Analysis

Let us consider a prefractal boundary $\partial\Omega$ of minimal cut-off ℓ characterizing its smallest geometrical features. It means that any geometrical detail of a

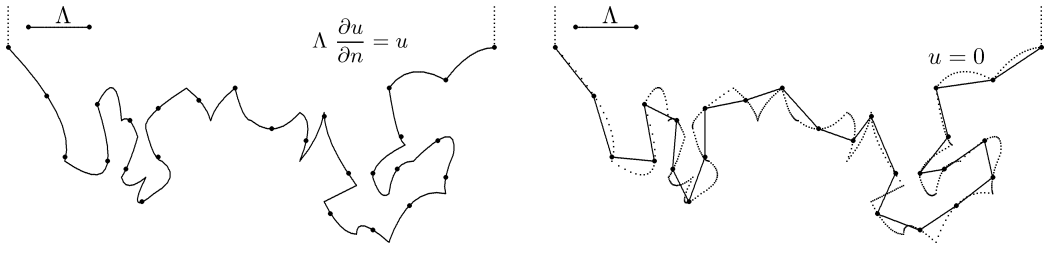

Fig. 2 Land Surveyor Approximation: the total flux across the boundary can be approximately calculated when the mixed boundary condition on a given irregular curve (on the left) is replaced by the Dirichlet condition $u = 0$ on the coarse-grained boundary (on the right). The last one is obtained by replacing curvilinear intervals of length Λ by corresponding linear chords.

smaller scale, if present, is supposed to be irrelevant. In particular, one may think that this prefractal curve is composed of linear segments of length ℓ. To study the scaling properties of the spread harmonic measures, one can use the ordinary methods of the multifractal analysis.[3] For these purposes, one takes a cover of the boundary $\partial\Omega$ by a finite number of disjoint compact sets Γ_k^δ (e.g. squares, disks, triangles) of a given diameter δ. The spread harmonic measure $\omega_{x,\Lambda}$ is then represented on scale δ by a finite number of probabilities $p_k(\Lambda,\ell,\delta) = \omega_{x,\Lambda}\{\partial\Omega \cap \Gamma_k^\delta\}$ satisfying the normalization condition: $\sum_k p_k(\Lambda,\ell,\delta) = 1$. For convenience, we use such covers that all probabilities $p_k(\Lambda,\ell,\delta)$ are strictly positive. In what follows, the starting point x, considered as a fixed parameter, will be omitted.

The scaling properties of the spread harmonic measures on a given scale δ are characterized by the moments

$$\zeta_q(\Lambda,\ell,\delta) = \sum_k [p_k(\Lambda,\ell,\delta)]^q \quad (q \in \mathbb{R})$$

and their local exponents

$$\tau_q(\Lambda,\ell,\delta) = \frac{\ln \zeta_q(\Lambda,\ell,\delta)}{\ln(\delta/L)} \qquad (5)$$

where L is the diameter of the whole boundary. In the case of the harmonic measure ($\Lambda = 0$) on fractal boundaries without cut-off ($\ell = 0$), the moments follow power laws with different *multifractal exponents* τ_q: $\zeta_q(\Lambda = 0, \ell = 0, \delta) \propto (\delta/L)^{\tau_q}$, as δ goes to 0. A similar scaling behavior with other exponents, $D_0(q-1)$, is known for the Hausdorff measure ($\Lambda = \infty$). The following qualitative arguments will be applied to study the intermediate case of the spread harmonic measures on an arbitrary self-similar fractal in $\mathbb{R}^2$ satisfying the local accessibility condition.

3.3. Qualitative Arguments

The moments $\zeta_q(\Lambda,\ell,\delta)$ involve three independent lengths: parameter Λ controlling the size of the CAR, minimal cut-off ℓ of the (pre)fractal boundary, and scale δ at which the spread harmonic measures are looked.

Let $\ell(\Lambda)$ denote the *diameter* of the characteristic absorption region. Since this region is a part of the prefractal curve, its diameter and perimeter are related by a scaling law with the Hausdorff dimension D_0:

$$\ell(\Lambda) \simeq \ell\ (\Lambda/\ell)^{1/D_0}.$$

First, let us investigate the possible ranges of the parameter Λ (Fig. 3). If $\Lambda < \ell$, the Brownian motion arrived on any linear segment (or other "elementary" part) of the boundary $\partial\Omega$ is mainly absorbed therein ($\ell(\Lambda) \ll \ell$). Consequently, the spread harmonic measure scarcely differs from the harmonic measure. Inversely, when Λ exceeds the total perimeter $L_{tot} \simeq \ell(L/\ell)^{D_0}$ of the boundary, the whole curve absorbs the partially reflected Brownian motion almost uniformly leading to the Hausdorff measure behavior. The most interesting case corresponds to values of Λ between ℓ and L_{tot}.

Although the scale δ formally varies from 0 up to infinity, non-trivial scaling results can be observed only for the range $\ell \ll \delta \ll L$ (Figs. 4b and 4c). Indeed, taking smaller scales than the minimal cut-off ℓ, one tries to study the distribution of the spread harmonic measure on such geometrical details which were supposed to be *irrelevant* (Fig. 4a). The values $\delta \gtrsim L$ are meaningless since the corresponding cover consists of a single set Γ_1^δ containing the whole studied curve. Assuming that the strong inequalities $\ell \ll \delta \ll L$ hold, one can distinguish three *scaling zones* shown schematically

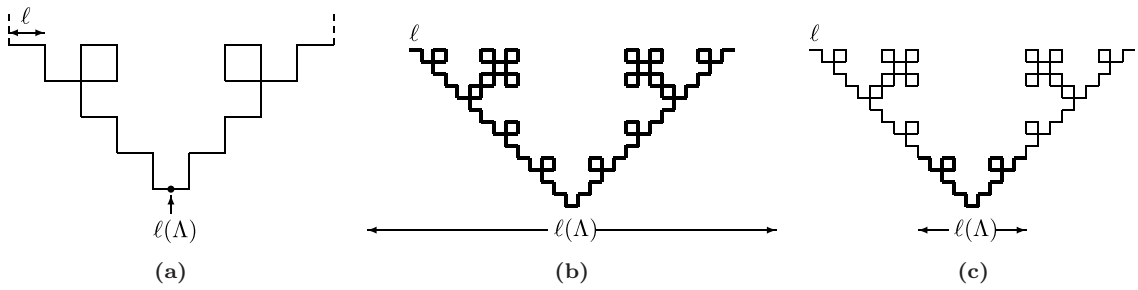

Fig. 3 Characteristic absorption region (drawn in bold) for different ranges of the parameter Λ: **(a)** for $\Lambda \ll \ell$, this region is too small with respect to the self-similar structure of the prefractal curve, so that the harmonic measure is almost not spread; **(b)** in the opposite case $\Lambda \gg L_{tot}$, the distribution of the absorption points is almost uniform on the whole curve; and **(c)** the most interesting situation corresponds to the intermediate range $\ell \ll \Lambda \ll L_{tot}$.

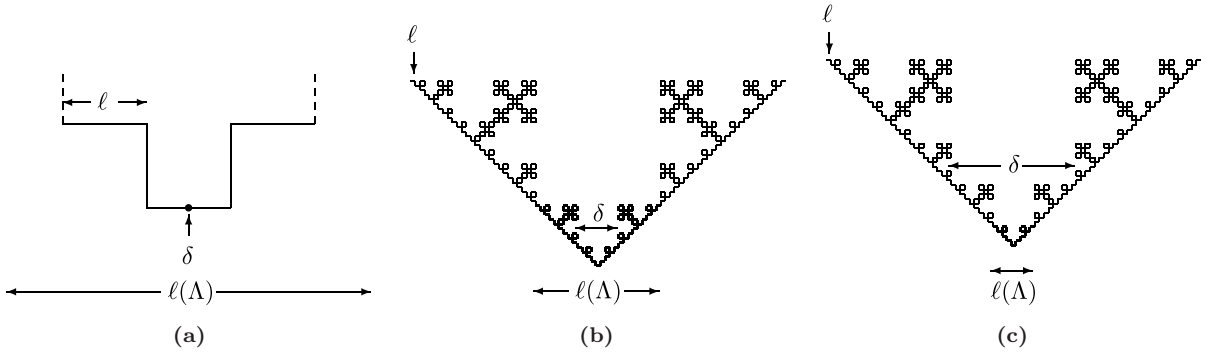

Fig. 4 Different ranges of the scale δ (for a fixed parameter $\ell \ll \Lambda \ll L_{tot}$): **(a)** for very small scales, one tries to consider irrelevant geometrical details; **(b)** for moderate scales, one investigates almost uniform distribution of the spread harmonic measure onto the characteristic absorption region (zone of the Hausdorff measure); and **(c)** for large scales, the characteristic absorption region is too small, so that the spread harmonic measure behaves like the harmonic measure on a coarse-grained generation (with the smallest segment length δ). The case of intermediate scales of order of $\ell(\Lambda)$ corresponds to the transition between the Hausdorff and harmonic measures. In all these cases, the characteristic absorption region is drawn in bold.

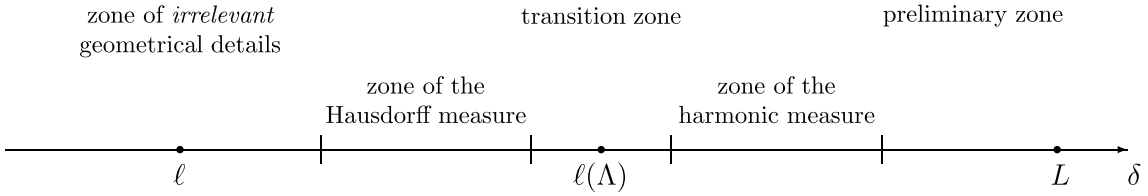

Fig. 5 Schematic representation of scale zones of the spread harmonic measure.

on Fig. 5:

- *Zone of the Hausdorff measure*: $\ell \ll \delta \ll \ell(\Lambda)$
  After the first hit to the boundary, the Brownian motion will be reflected many times, staying mainly in the characteristic absorption region. It means that the absorption probabilities on this region are distributed uniformly in a first approximation, and the spread harmonic measure behaves like the Hausdorff measure:
  $$\tau_q(\Lambda, \ell, \delta) \simeq D_0(q-1).$$
- *Zone of transition between Hausdorff and harmonic measures*: $\delta \propto \ell(\Lambda)$
  This zone provides a new feature in scaling behavior. Actually, it represents the transitional state between the harmonic and Hausdorff measures. In particular, we shall show in Sec. 5 that this region is responsible for the CPA frequency response of (pre)fractal boundaries.
- *Zone of the harmonic measure*: $\ell(\Lambda) \ll \delta \ll L$
  In this case, the absorption region is too small with respect to the scale δ, and the spread harmonic measure scales like the harmonic measure on the generation with the smallest segment length δ. Since δ is still sufficiently smaller than the diameter L of the whole prefractal curve, one finds the multifractal exponents of the harmonic measure:
  $$\tau_q(\Lambda, \ell, \delta) \simeq \tau_q.$$

The preceding analysis was completely based on the relation between the scale δ and the diameter $\ell(\Lambda)$ of the characteristic absorption region. Consequently, the local exponents $\tau_q(\Lambda, \ell, \delta)$ are determined only by the ratio $\delta/\ell(\Lambda)$ that can be written as:

$$\tau_q(\Lambda, \ell, \delta) \equiv \tau_q(\xi) \quad \text{with } \xi = \ln \frac{\delta}{\ell(\Lambda)} \tag{6}$$

where the dependence on Λ, ℓ and δ is represented via the only *scaling parameter* ξ. We conclude that the scaling behavior of the spread harmonic measures is entirely described by a set of quantities $\tau_q(\xi)$ (parametrized by q) which can be called *multifractal exponent functions*. We remind that the scaling properties of the harmonic measure were determined by a set of multifractal exponents τ_q, while the characterization of the Hausdorff measure required the only dimension D_0 since the corresponding multifractal exponents were $D_0(q-1)$. Being more sophisticated objects, the spread harmonic measures necessitate more information to be described.

3.4. Scaling Parameter

The scaling parameter ξ plays an important role representing the dependence of local exponents through the main length parameters of the problem: scale δ, length Λ and minimal cut-off ℓ. In particular, it allows to study the influence of each of them independently or in combination.

As we have seen, the multifractal exponent functions $\tau_q(\xi)$ possess two asymptotic limits $D_0(q-1)$ and τ_q for small and large ξ, respectively. Consequently, an increase of the scale δ from ℓ to L provides a continuous transition between the Hausdorff and harmonic measures.

The most interesting dependence is related to the parameter Λ which can be freely modified from 0 up to infinity. Taking Λ from the minimal cut-off ℓ (smallest segment length) to the total perimeter L_{tot} of the whole curve, one can reconstruct the multifractal exponent functions $\tau_q(\xi)$ showing again a continuous transition between the harmonic measure ($\Lambda = 0$) and the Hausdorff measure ($\Lambda = \infty$). The fact that the values of the multifractal exponents can be controlled by the physical parameter Λ opens promising perspectives for optimal geometry design of efficient catalysts in chemical engineering.

Finally, one can examine the dependence on the minimal cut-off ℓ for fixed Λ and δ. Since a decrease of ℓ leads to the decrease of the diameter $\ell(\Lambda)$ and, consequently, to the growth of the scaling parameter ξ, the spread harmonic measures become closer and closer to the harmonic measure. Formally proceeding the limit of a fractal boundary ($\ell \to 0$ with fixed δ and Λ), one obtains the harmonic measure which can thus be thought of as a trivial extension of the spread harmonic measures on really fractal boundaries. In Sec. 6, we shall discuss another extension preserving the main properties of the spread harmonic measures.

4. NUMERICAL SIMULATIONS

4.1. Geometry-Adapted Fast Random Walk Algorithm

Except a few particular cases, the spread harmonic measures are not known explicitly. Therefore, we are going to model the Brownian motion reflected with jump in order to calculate its absorption probability density $\omega^{(a)}_{x,\Lambda}(s)$ for a given boundary $\partial\Omega$. As we have seen, its scaling properties in the limit $a \to 0$ correspond to those of the spread harmonic measure.

The simulation of the Brownian motion reflected with jump is carried out with the help of the fast random walk algorithm adapted to the quadratic Koch curve.[23,24] For a given parameter Λ, one chooses a small jump distance a and calculates the sticking probability σ according to (3). For a fixed starting point x, one considers a circle which *does not intersect* the boundary $\partial\Omega$. The hierarchical structure of the self-similar quadratic Koch curve allows one to construct this circle in an efficient way (see Ref. 23 for details). To hit the boundary, the Brownian motion must intersect this circle at random point x' distributed uniformly on this circle due to its rotational symmetry. This technique permits one to replace long time-consuming simulations of the Brownian motion inside the circle by a single jump to the circle point x'. Starting from this point, one constructs a new circle which does not intersect the boundary, and so on. When the distance between the current position of the Brownian motion and the boundary becomes less than a chosen threshold, the motion is thought to be arrived on the boundary (in vicinity of some boundary point s). After that, the process is stopped with probability σ (absorption at point s), or it is continued from the neighboring point $s + an(s)$ with probability $(1 - \sigma)$. In the last case, one employs the above technique to model the Brownian motion until the next hit to the boundary, and so on. Numerous repetition of the algorithm allows one to compute the absorption probability density $\omega^{(a)}_{x,\Lambda}(s)$. Reproducing these simulations for smaller and smaller values of the jump distance a, one can check how close these densities are to their limit $\omega_{x,\Lambda}(s)$. The simulations are terminated when the spread harmonic measure density $\omega_{x,\Lambda}(s)$ is obtained with desired accuracy.

4.2. Numerical Results

The most important result that we are going to check is the universality of the multifractal exponent functions $\tau_q(\xi)$. In other words, we ought to verify that these functions are the intrinsic characteristics of the spread harmonic measures on a chosen type of geometry, independently of the minimal cut-off ℓ, scale δ and length Λ. For these purposes, the spread harmonic measure density has been calculated numerically in 12 cases. For each generation order $g = 5, 6, 7, 8$ (with corresponding minimal cut-off $\ell_g = L(1/3)^g$), we took three values $\Lambda_m = 10^{-m}L$, with $m = 1, 2, 3$. Once the

probabilities $\{p_k(\Lambda_m, \ell_g, \delta)\}$ are determined by the geometry-adapted fast random walk algorithm, we computed the moments $\zeta_q(\Lambda_m, \ell_g, \delta)$ and the corresponding local exponents $\tau_q(\Lambda_m, \ell_g, \delta)$ on different scales δ from ℓ_g to $L/3$, taking for convenience discrete values $\delta_n = L(1/3)^n$ with $n = 1, 2, \ldots, g$.

As a typical case, we consider the second moment $\zeta_2(\Lambda_m, \ell_g, \delta)$. According to the above scheme, we obtain 12 dependencies of the local correlation exponent $\tau_2(\Lambda_m, \ell_g, \delta)$ as a function of the scale δ. If the preceding analysis is valid, all these dependencies should fall onto the same curve $\tau_2(\xi)$ drawn versus the only scaling parameter ξ. Figure 6 shows several of these dependencies. A good collapse of the numerical data confirms the validity of the above qualitative arguments. In particular, one can see the predicted scaling behavior: for small ξ ($\xi < -1$), there is the asymptotic level at $\tau_2(\xi) \approx 1.465$ corresponding to the Hausdorff measure. For large ξ ($\xi > 4$), $\tau_2(\xi)$ descends to 1 and even lower (see the eighth generation), to the correlation exponent τ_2 of the harmonic measure: $\tau_2(\xi) \approx 0.89$ (see Ref. 23). The numerical simulations justify thus the introduction of the multifractal exponent functions $\tau_q(\xi)$ to describe the scaling properties of the spread harmonic measures.

5. CONSTANT PHASE ANGLE BEHAVIOR

The spread harmonic measures have been introduced as a natural description of transfer capacities

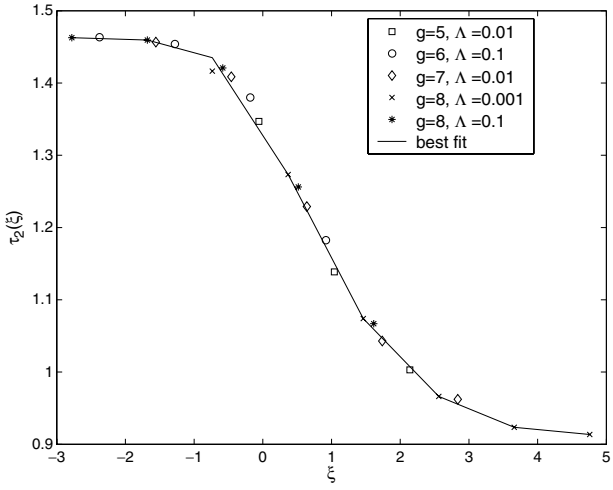

Fig. 6 Local exponents $\tau_2(\Lambda, \ell, \delta)$ of the spread harmonic measures on different generations $g = 5, 6, 7, 8$ of the quadratic Koch curve with different $\Lambda_m = 10^{-m}L$ ($m = 1, 2, 3$). All these dependencies, considered as functions of the scaling parameter $\xi = \ln(\delta/\ell(\Lambda))$, fall onto the same curve $\tau_2(\xi)$ referred to as the correlation exponent function of the spread harmonic measures.

of a partially absorbing (semi-permeable) boundary. To illustrate its practical applications, we are going to use the underlying concepts to reveal the anomalous frequency dependence of the spectroscopic impedance for irregular morphologies.

A linear response of an electrolytic cell composed of two metallic electrodes placed into an electrolyte can be characterized by the impedance $Z_{cell}(\omega)$ depending on the frequency ω of the applied electric potential. This quantity represents the bulk resistance of the electrolyte (constant term) and the transport characteristics of the ionic double layer near metallic electrodes. The last term $Z(\omega)$ corresponding to the boundary response is called spectroscopic impedance. If one considers a flat metallic surface, the ionic double layer oughts to behave like a capacitor of the surface capacitance γ: $Z(\omega) = (-i\gamma\omega)^{-1}$. In practice, however, the spectroscopic impedance remains inversely proportional to the frequency only in asymptotic regimes of very high or very low frequencies. For an intermediate frequency range, the surface roughness leads to *anomalous frequency behavior*.[25–27] The most typical dependence is given by the power law $Z(\omega) \propto (-i\gamma\omega)^{-\beta}$ and called *constant phase angle behavior* (CPA). A lot of theoretical, numerical and experimental works have been addressed to the problem of how the physical exponent β can be related to the roughness of the boundary.[9,15,28–36] For self-similar fractal boundaries in the plane, two expressions have been derived: the simplified relation[28–30]

$$\beta = \frac{1}{D_0} \tag{7}$$

and the more accurate one[15,32]

$$\beta = \frac{\tau_2}{D_0}. \tag{8}$$

We remind that D_0 is the Hausdorff dimension of the fractal, while τ_2 is the correlation exponent of the harmonic measure on the boundary. In what follows, we are going to retrieve these relations in terms of the preceding study of the spread harmonic measure. The present approach will then provide a new understanding of these results.

The following analysis is based on the simple expression for the spectroscopic impedance derived by Filoche and Sapoval.[10] In present notations, the spectroscopic impedance on scale δ can be written as $Z(\omega) = \rho\Lambda\ z(\Lambda, \ell, \delta)$, where

$$z(\Lambda, \ell, \delta) = \sum_k p_k(\Lambda, \ell, \delta)\ p_k(\Lambda = 0, \ell, \delta),$$

ρ is the electrolyte resistivity and Λ is inversely proportional to the frequency ω (for details, see Ref. 18). In the fractal regime ($\ell \ll \delta \ll L$), the sum $z(\Lambda, \ell, \delta)$ follows a power law

$$z(\Lambda, \ell, \delta) \propto (\delta/L)^{\gamma(\Lambda,\ell,\delta)} \tag{9}$$

with some local exponent $\gamma(\Lambda, \ell, \delta)$ depending on Λ, ℓ and δ. As previously, one expects to encounter three scaling zones:

- On small scales, the spread harmonic measure behaves like the Hausdorff measure, therefore
$$\gamma(\Lambda, \ell, \delta) \simeq D_0.$$
- On intermediate scales, one faces a transition zone with a non-trivial behavior.
- On large scales, the spread harmonic measure scarcely differs from the harmonic measure, and the sum $z(\Lambda, \ell, \delta)$ is then close to the second moment $\zeta_2(\Lambda = 0, \ell, \delta)$, whence
$$\gamma(\Lambda, \ell, \delta) \simeq \tau_2.$$

As for the moments of the spread harmonic measure, the function $\gamma(\Lambda, \ell, \delta)$ depends entirely on the only scaling parameter $\xi = \ln(\delta/\ell(\Lambda))$:

$$\gamma(\Lambda, \ell, \delta) \equiv \gamma(\xi)$$
$$\text{with } \xi = \ln\left(\frac{\delta/L}{(\Lambda/L)^{1/D_0}\ (\ell/L)^{(1-1/D_0)}}\right) \tag{10}$$

where the diameter $\ell(\Lambda)$ is written in an explicit scaling form. Taking two close values Λ and Λ', one rewrites (9) as

$$\frac{z(\Lambda, \ell, \delta)}{z(\Lambda', \ell, \delta)} \simeq \exp([\gamma(\xi) - \gamma(\xi')] \ln \delta/L).$$

On the other hand, for a fixed scale δ, one expects the CPA dependence on the parameter Λ:

$$\frac{z(\Lambda, \ell, \delta)}{z(\Lambda', \ell, \delta)} \simeq \left(\frac{\Lambda}{\Lambda'}\right)^{\beta(\delta,\ell)-1}$$

with some local exponent $\beta(\delta, \ell)$ depending on δ and ℓ. By equalling these expressions, one obtains

$$\beta(\delta, \ell) \simeq 1 + [\gamma(\xi) - \gamma(\xi')]\ \frac{\ln \delta/L}{\ln \Lambda/\Lambda'} \tag{11}$$

where ξ and ξ' are related to δ, ℓ, Λ and Λ' by (10).

For small scaling parameters ξ and ξ', function $\gamma(\xi)$ does not almost vary being close to D_0. Thus, the difference in square brackets is almost 0, i.e. $\beta(\delta, \ell) \simeq 1$. So, we have obtained the zone of the Hausdorff measure corresponding to the low frequency asymptotic regime of the impedance behavior. Similarly, when the scaling parameters ξ and ξ' are large, function $\gamma(\xi)$ is close to τ_2, and one finds again $\beta(\delta, \ell) \simeq 1$ corresponding to the zone of the harmonic measure and related to the high frequency asymptotic regime.

The most interesting behavior is found for the transition zone. Let us assume for a moment that $\gamma(\xi)$ can be approximated by a linear function: $\gamma(\xi) \simeq \gamma_0 + \gamma_1 \xi$. The coefficient γ_1 is given by two crossovers ξ_{min} and ξ_{max} corresponding to the low and high frequency asymptotic regimes (see Fig. 7):

$$\gamma_1 \simeq \frac{D_0 - \tau_2}{\xi_{min} - \xi_{max}} = \frac{D_0 - \tau_2}{(1/D_0)\ln(\Lambda_{min}/\Lambda_{max})}. \tag{12}$$

On the scale δ, the studied prefractal curve looks like a generation with the smallest segment length of order of δ, whence $\Lambda_{min} \simeq \delta$. The perimeter of this generation can be written as $\delta\ (L/\delta)^{D_0}$, leading to $\Lambda_{max} \simeq \delta\ (L/\delta)^{D_0}$. Substituting these relations in (12), one has

$$\gamma_1 \simeq \frac{D_0 - \tau_2}{\ln \delta/L} \quad \text{and} \quad \beta(\delta, \ell) \simeq 1 - \gamma_1 \frac{\ln \delta/L}{D_0} \simeq \frac{\tau_2}{D_0}.$$

We have retrieved the relation of Halsey and Leibig[15] between the impedance exponent β, the correlation exponent τ_2 of the harmonic measure, and the Hausdorff dimension D_0 of the fractal boundary.

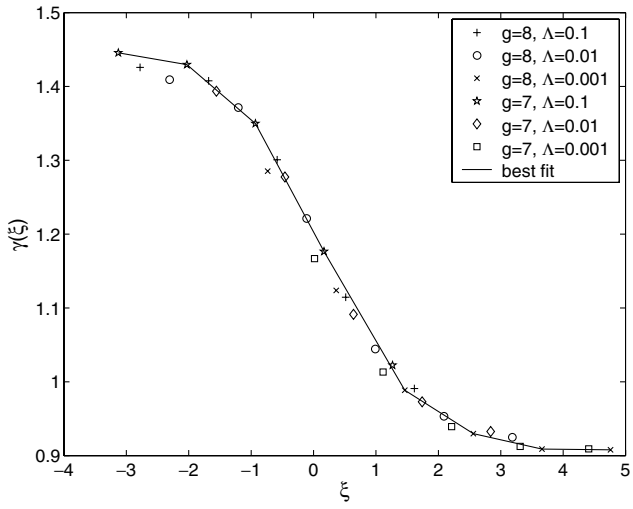

Fig. 7 Function $\gamma(\xi)$ calculated for generations $g = 7$ and $g = 8$ of the quadratic Koch curve. Six curves correspond to different values of $\Lambda_m = 10^{-m}L$ ($m = 1, 2, 3$), while the scaling parameter $\xi = \ln(\delta_n/\ell(\Lambda))$ takes several values with $\delta_n = (1/3)^n L$ ($n = 1, \ldots, g$). For the sake of clarity, only reference points are shown. One can see that these points fall onto the same universal curve $\gamma(\xi)$. One also finds two asymptotic levels at $D_0 \approx 1.465$ and $\tau_2 \approx 0.89$ corresponding to the low and high frequency regimes of the spectroscopic impedance. The intermediate fractal regime between two crossovers can be approximated by a linear function.

The above analysis was based on the assumption that the boundary was a sufficiently high generation of a fractal. In particular, relation (8) was obtained as linear interpolation between *well-established* zones of the Hausdorff and harmonic measures. In practice, however, one usually deals with the first generations of a fractal. The most experiments have been realized on finite generations of order between 1 and 5. Being defined on such boundaries, the spread harmonic measures exhibit *prefractal* scaling properties, i.e. they scale in a non-trivial way, but with exponents that did not achieve the expected well-established values. Similarly, studying the impedance behavior for the first generations of a fractal, one can find the prefractal regime with a certain exponent β'. This value would be larger than β given by relation (8). In order to explain this discrepancy, we consider again the linear approximation of the function $\gamma(\xi)$ in prefractal regime for the first generations. In this case, the zone of the harmonic measure is not yet well-established. One should thus replace the correlation exponent τ_2 in relation (12) by 1 (the value of this exponent for a smooth boundary) that leads to the simplified relation (7).

In the light of the above remarks, it is not surprising that numerical simulations and physical experiments with blocking electrodes (e.g. reported in Ref. 35) confirmed the simplified relation (7), since these researches were carried out for the first generations of a fractal boundary. For higher generations, the impedance exponent β would be given by (8). At the same time, both relations (7) and (8) correspond to a linear interpolation of the function $\gamma(\xi)$ in the transition zone. The whole function $\gamma(\xi)$ provides the complete information about scaling properties of the spectroscopic impedance which is required, in particular, to study crossovers between classical and fractal regimes.

6. CONJECTURAL EXTENSION TO FRACTAL BOUNDARIES

We have seen in Subsec. 3.3 that a formal attempt to pass to really fractal curves (limit $\ell \to 0$) leads to the (ordinary) harmonic measure. The main inconvenience of such *trivial* extension that the spread harmonic measures become independent of Λ, and they scale with classical multifractal exponents τ_q instead of multifractal exponent functions $\tau_q(\xi)$. In particular, the spreading effect, the most interesting feature of these measures, would be suppressed in the limit $\ell \to 0$. In this section, we propose a *conjectural* extension of the spread harmonic measures to really fractal boundaries that preserves their main properties.

For real fractals, the notion of curvilinear distance becomes invalid. Indeed, if one considers a part of a fractal curve between any two distinct points, its perimeter, even if defined, is infinite. In particular, the characteristic absorption region of a *fixed perimeter* Λ becomes meaningless for real fractals. In this light, a reasonable measure of *proximity* between two distinct points on a fractal curve is the Euclidean distance between them. The idea is then to introduce the partially reflected Brownian motion in a such way that the fixed parameter Λ will correspond to a specific Euclidean distance on the fractal. The *diameter* of the characteristic absorption region seems to be an appropriate candidate.

For a given positive length Λ, let us proceed again the construction of the Brownian motion reflected with jump on a prefractal curve of minimal cut-off ℓ. As previously, the (ordinary) Brownian motion is started from a given interior point $x \in \Omega$. After the hitting of the boundary, the diffusing particle can be absorbed with probability σ, or it is reflected by jump to a neighboring point within a small distance a with probability $(1-\sigma)$. The motion continues until the absorption. The spread harmonic measure was obtained from the corresponding absorption distributions in the double limit $a \to 0$ and $\sigma \to 0$, being related by (3).

The new feature here is that the jump distance a, the sticking probability σ, and the minimal cut-off ℓ have to vanish simultaneously. The question is how fast one of these parameters goes to 0 with respect to the others. The dimension analysis suggests to choose the jump distance a to be of order of the minimal cut-off ℓ, i.e. $a \propto \ell$. In the preceding construction in Sec. 2, the mixed boundary condition implied that the jump distance a and the sticking probability σ were of the same order: $a/\sigma \simeq \Lambda$. Since the perimeter L_{abs} of the characteristic absorption region was also of order of a/σ, one had $L_{abs} \propto \Lambda$. Now, we would like to construct the Brownian motion reflected with jump in such a way that the *fixed parameter* Λ represents the *diameter* $\ell(\Lambda)$ of the characteristic absorption region. Since this region is a part of the (pre)fractal curve, its perimeter a/σ and diameter Λ are related by the scaling law $a/\sigma \simeq \ell\ (\Lambda/\ell)^{D_0}$, whence

$$\sigma \simeq (a/\Lambda)^{D_0} \quad (a \to 0). \tag{13}$$

This relation can be thought as a conjectural representation of the mixed boundary condition for really fractal boundaries. Since the relation $\ell(\Lambda) \simeq \Lambda$ is now independent of the minimal cut-off ℓ, it is valid even for a real fractal (i.e. in the limit $\ell \to 0$). The spread harmonic measures obtained in this limit would be described by the same multifractal exponent functions $\tau_q(\xi)$ as in the case of prefractal curves with a given minimal cut-off ℓ. The scaling parameter ξ becomes now equal to $\ln(\delta/\Lambda)$. We stress that the existence of the limit remains an open mathematical question.

7. CONCLUSION

The family of the spread harmonic measures associated to the mixed boundary problem (2) has been introduced as an efficient mathematical tool to describe the transfer capacity of different subsets of a partially absorbing (semi-permeable) boundary. The scaling properties of the spread harmonic measures have been studied on self-similar fractals satisfying the local accessibility condition. In the case of prefractal curves, we have shown that these properties were completely determined by a set of multifractal exponent functions $\tau_q(\xi)$. These functions had two asymptotic levels at τ_q and $D_0(q-1)$ corresponding to the zones of the harmonic and Hausdorff measures respectively, while intermediate values of ξ presented a transition zone. Variation of the parameter Λ from 0 up to infinity realized a continuous transition between the harmonic measure ($\Lambda = 0$) and the Hausdorff measure ($\Lambda = \infty$).

The dependence of the multifractal exponent functions $\tau_q(\xi)$ on the main lengths of the problem, namely, parameter Λ, scale δ and minimal cut-off ℓ, was represented via the only scaling parameter ξ. In other words, the multifractal exponent functions were shown to be the intrinsic characteristics of the family of the spread harmonic measures. Once the functions $\tau_q(\xi)$ were determined for a given type of fractal boundary, the scaling properties of the spread harmonic measures could be obtained for any scale, any minimal cut-off and any length Λ by a simple variation of the scaling parameter ξ. Moreover, the invariance of the multifractal exponent functions with respect to the minimal cut-off ℓ allowed us to propose a conjectural extension of the spread harmonic measures on really fractal boundaries (limit $\ell \to 0$).

As a typical fractal boundary, we have considered the quadratic Koch curve of the Hausdorff dimension $D_0 = \ln 5/\ln 3$. The implementation of the geometry-adapted fast random walk algorithm allowed us to calculate numerically the moments of the spread harmonic measures on different scales. In particular, the local correlation exponents $\tau_2(\Lambda, \ell, \delta)$ have been computed for several generation orders g, scales δ and lengths Λ. Their values plotted versus the scaling parameter ξ fell precisely onto the same curve, namely, the correlation exponent function $\tau_2(\xi)$. This result provided an accurate numerical verification of the developed qualitative arguments.

Finally, a close relation between the spectroscopic impedance of the working electrode and the spread harmonic measures suggested an idea to apply the present scaling analysis to reveal the relation between the CPA exponent β and the surface roughness. To characterize how the spectroscopic impedance scales, we introduced the function $\gamma(\xi)$ exhibiting two asymptotic limits corresponding to the zones of the Hausdorff and harmonic measures. A simple linear interpolation of this function at the intermediate zone led to the classical relation (8) between CPA exponent β, fractal dimension D_0 and correlation exponent τ_2 of the harmonic measure. It was stressed that the complete function $\gamma(\xi)$ provided a more accurate description required to study the crossovers between different regimes. Moreover, it revealed a small distinction between the simplified relation (7) and more accurate relation (8) for the CPA exponent, and allowed us to explain the related disagreements in literature.

ACKNOWLEDGMENTS

The author thanks Professors M. Filoche, P. Jones, N. Makarov, B. Sapoval and W. Werner for valuable discussions on the subject.

REFERENCES

1. B. Mandelbrot, *The Fractal Geometry of Nature* (Freeman, San Francisco, 1982).
2. J. B. Garnett and D. E. Marshall, *Harmonic Measure* (Cambridge University Press, Cambridge, 2005).
3. P. Meakin, *Fractals, Scaling and Growth Far from Equilibrium* (Cambridge University Press, 1998).
4. K. J. Falconer, *Fractal Geometry: Mathematical Foundations and Applications* (John Wiley and Sons, Chichester, 1990).
5. T. A. Witten and L. M. Sander, *Phys. Rev. Lett.* **47** (1981) 1400–1403.

6. D. A. Kessler, J. Koplik and H. Levine, *Adv. Phys.* **37** (1988) 255–339.
7. L. D. Landau and E. M. Lifshitz, *Theoretical Physics: Electrodynamics of Continuous Media* (Pergamon Press, Oxford, London, New York, 1960).
8. B. Sapoval, *Phys. Rev. Lett.* **73** (1994) 3314–3316.
9. B. Sapoval, in *Fractals and Disordered Systems*, eds. A. Bunde and S. Havlin (Springer, 1996) p. 233.
10. M. Filoche and B. Sapoval, *Eur. Phys. J. B* **9** (1999) 755–763.
11. S. Kakutani, *Imp. Acad. Tokyo* **20** (1944) 706–714.
12. D. S. Grebenkov, in *Focus on Probability Theory*, Vol. 1, ed. L. R. Velle (Nova Science Publishers Inc., 2006).
13. M. Felici, M. Filoche, C. Straus, T. Similowski and B. Sapoval, *Resp. Phys.* **145** (2005) 279–293.
14. D. S. Grebenkov, M. Filoche, B. Sapoval and M. Felici, *Phys. Rev. Lett.* **94** (2005) 050602-1–050602-4.
15. T. C. Halsey and M. Leibig, *Ann. Phys.* **219** (1992) 109–147.
16. M.-O. Coppens, *Catalysis Today* **53** (1999) 225–243.
17. J. S. Andrade Jr., M. Filoche and B. Sapoval, *Europhys. Lett.* **55**(4) (2001) 573–579.
18. D. S. Grebenkov, Laplacian transport towards irregular interfaces: a theoretical, numerical and experimental study, PhD thesis, Ecole Polytechnique, France (2004).
19. D. S. Grebenkov, M. Filoche and B. Sapoval, *Eur. Phys. J. B* **36**(2) (2003) 221–231.
20. R. F. Anderson and S. Orey, *Nagoya Math. J.* **60** (1976) 189–216.
21. M. Freidlin, *Functional Integration and Partial Differential Equations*, Annals of Mathematics Studies (Princeton University Press, Princeton, New Jersey, 1985).
22. M. Filoche and B. Sapoval, *J. Phys. I France* **7** (1997) 1487–1498.
23. D. S. Grebenkov, A. A. Lebedev, M. Filoche and B. Sapoval, *Phys. Rev. E* **71** (2005) 056121-1–056121-11.
24. D. G. Grebenkov, *Phys. Rev. Lett.* **95** (2005) 200602-1–200602-4.
25. R. de Levie, *Electrochim. Acta* **10** (1965) 113–130.
26. W. Scheider, *J. Phys. Chem.* **79** (1975) 127–136.
27. R. D. Armstrong and R. A. Burnham, *J. Electroanal. Chem.* **72** (1976) 257–266.
28. A. Le Mehaute and G. Crepy, *Solid State Ionics* **9&10** (1983) 17–30.
29. L. Nyikos and T. Pajkossy, *Electrochim. Acta* **30**(11) (1985) 1533–1540.
30. P. Meakin and B. Sapoval, *Phys. Rev. A* **43** (1991) 2993–3004.
31. S. H. Liu, *Phys. Rev. Lett.* **55** (1985) 529–532.
32. T. C. Halsey, *Phys. Rev. A* **35** (1987) 3512–3521.
33. M. Leibig and T. C. Halsey, *J. Electroanal. Chem.* **358** (1993) 77–109.
34. A. E. Larsen, D. G. Grier and T. C. Halsey, *Phys. Rev. E* **52**(RC) (1995) R2161–R2164.
35. B. Sapoval, R. Gutfraind, P. Meakin, M. Keddam and H. Takenouti, *Phys. Rev. E* **48** (1993) 3333–3344.
36. H. Ruiz-Estrada, R. Blender and W. Dieterich, *J. Phys. Condens. Matter* **6** (1994) 10509–10517.